



Factors influencing chemical relative potency in mixture toxicity risk assessment

Frances Widjaja-van den Ende

The concept of relative potency (REP) is well established through terms like REP, relative potency factor (RPF), and toxic equivalency factor (TEF). REP is often determined using *in vivo* data, such as for dioxins. However, many factors such as dose, species, endpoint, interindividual variability, and chemical structure can influence REP values. This mini review examines REP values for pyrrolizidine alkaloid N-oxides (PA-N-oxides) versus their parent alkaloids. Using physiologically based kinetic (PBK) model simulations, the impact of dose, species, endpoint, interindividual variability, and chemical structure on REP values could be quantified. Results show that interindividual variability and chemical structure are the most influential. This highlights PBK modeling as a valuable tool for predicting REP, especially when animal data are limited and *in vitro* tests alone are insufficient.

Addresses

Division of Toxicology, Wageningen University, Stippeneng 4, 6708 WE Wageningen, the Netherlands

Corresponding author: Widjaja-van den Ende, Frances (Frances1.widjaja@wur.nl)

Current Opinion in Toxicology 2025, **43**:100541

This review comes from a themed issue on **General Toxicology**

Edited by **Dr. José E. Manautou** and **Dr. Martin van den Berg**

Available online 30 June 2025

For a complete overview see the [Issue](#) and the [Editorial](#)

<https://doi.org/10.1016/j.cotox.2025.100541>

2468-2020/© 2025 The Author(s). Published by Elsevier B.V. This is an open access article under the CC BY license (<http://creativecommons.org/licenses/by/4.0/>).

Introduction

In modern food chain, one encounters combined exposure to chemicals from groups of compounds with similar structures, toxicokinetics, toxicodynamics, and mode of action. Examples are exposure to dioxins, perfluoroalkyl and polyfluoroalkyl substances (PFAS), or pyrrolizidine alkaloids (PAs) and their N-oxides (PA-N-oxides). Risk assessment of these combined exposures is preferably performed using the toxic equivalency concept, where combined exposure is expressed in terms of equivalents of a selected reference compound from the group. This implies that exposure to the mixture is quantified by adding up the dose levels of

each congener multiplied by its relative potency with respect to the reference compound, where the risk can be evaluated based on toxicity of the respective reference compound. The relative potencies of the chemicals are defined as relative potency (REP), relative potency factor (RPF), or toxic equivalency factor (TEF) [1,2], further referred to as REP in this review.

Defining REP requires toxicity data in an assay that reflects the critical adverse effect so that the values are defined for the relevant toxic endpoint. These assays may include *in vitro* assays, like the dioxin receptor-chemically-activated luciferase expression (DR-CALUX) quantifying Aryl hydrocarbon-receptor (Ah-receptor) activation for defining TEF values for dioxins [3], or *in vivo* data on liver toxicity that have been used to propose RPF for PFAS [4], although liver toxicity does not match the critical immune toxicity effect used by the European Food Safety Authority (EFSA) to define the tolerable weekly intake (TWI) for PFAS [5]. The use of these *in vitro* and *in vivo* assays defines the REP used in subsequent risk assessment of human dietary exposures to these groups of chemicals. Given that risk assessment of these combined exposures relates to the human situation, it indicates that REP should be relevant for human and at low realistic dose levels. This raises the question as to what extent species differences, concentrations or doses, and endpoint used, differences between *in vitro* and *in vivo*, or interindividual differences influence REP, and how these influences compare to the differences caused by the variation in chemical structure of the congeners.

The current review summarizes insights obtained by studying these questions for the group of PA-N-oxides and their parent PAs, comprising a group of natural toxins present in foods like honey, herbal teas, and food supplements [6].

Use of new approach methodologies

In vivo studies unlikely provide insights into the influence of dose, endpoint used, species differences, and interindividual differences on REP, given that such studies would require high numbers of experimental animals, cannot be done in humans, are hard to perform at realistic low dose levels given the sensitivity of the detection methods, and cannot define the

influence of human interindividual differences. Instead, new approach methodologies (NAMs), consisting of in silico and in vitro approaches, can be applied, and PAs and their N-oxides were selected as the model compounds. The toxicity of PA-N-oxides depends on their chemical reduction back to the parent PAs, which induce liver toxicity and liver carcinogenicity via formation of reactive pyrrole-intermediates that form protein and DNA adducts. This implies that the toxicity of the PA-N-oxides relative to their parent PAs can be quantified by quantifying the level of formation and internal exposure to the parent PA upon dosing the PA-N-oxide, as compared to the internal exposure to the parent PA upon dosing an equimolar dose of this parent PA. The relevant kinetic parameters, including the maximum blood concentration (C_{max}) and the area under the concentration-time curve from 0 to 24 h (AUC_{0-24h}) for the parent PA, can be defined by physiologically based kinetic (PBK) modeling [7]. Figure 1a provides the PBK model-based prediction of the blood concentration-time profile for riddelliine upon dosing rats with the parent PA riddelliine or with an equimolar dose of the related PA-N-oxide. The ratio of the PBK model-predicted area-under-the-riddelliine concentration-time curve ($AUC_{0-24h, RID}$) upon dosing riddelliine N-oxide compared to the $AUC_{0-24h, RID}$ upon an equimolar dose of riddelliine reflects the $REP_{RIDO \text{ to } RID}$ and amounts to 0.67 [7]. This value is in line with the $REP_{RIDO \text{ to } RID}$ of 0.64 derived from available in vivo data on the amount of riddelliine-derived DNA adducts/ 10^8 nucleotides in the liver of rats exposed to riddelliine or riddelliine N-oxide [8], indicating the validity of the NAMs applied, and supporting that PBK modeling

provides a way to define in vivo $REP_{PANO \text{ to } PA}$ without animal experiments.

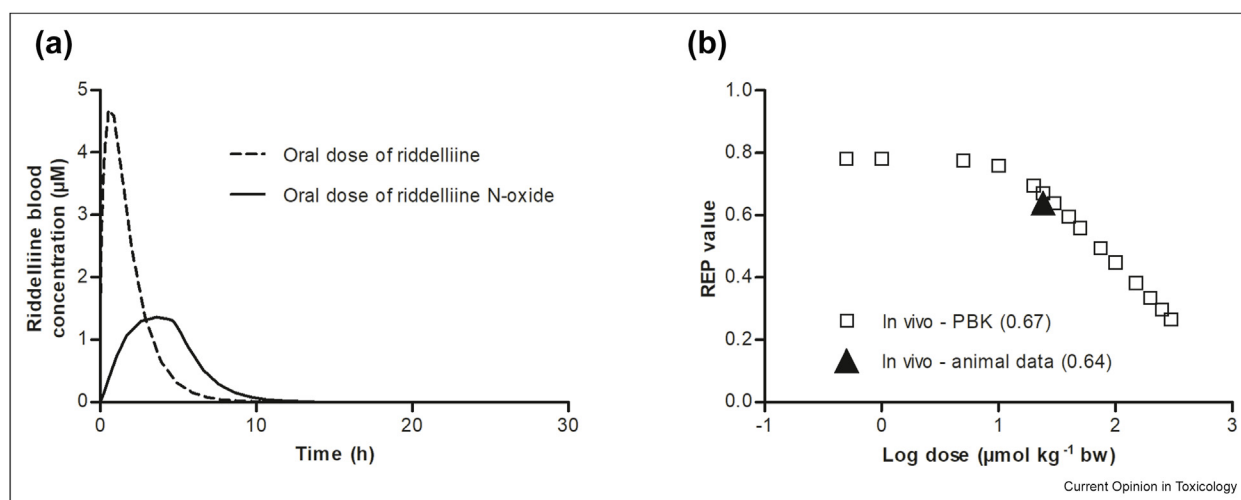
Effect of dose

The PBK model developed for riddelliine and riddelliine N-oxide in rats also facilitates definition of concentration-time curves for riddelliine in rats at doses other than the one used in the available in vivo experiment (Figure 1a). This allows evaluating the effect of dose on $REP_{RIDO \text{ to } RID}$. Figure 1b shows that $REP_{RIDO \text{ to } RID}$ depends on the dose, with the value of 0.67 obtained at 8.8 mg/kg bw riddelliine N-oxide and 8.4 mg/kg bw riddelliine (both 24 $\mu\text{mol/kg}$ bw), increasing with decreasing dose and reaching a constant value of 0.78 at dose levels below 1 $\mu\text{mol/kg}$ bw [7]. The PBK model also highlights that this effect of increasing dose on the decreasing $REP_{RIDO \text{ to } RID}$ value is due to saturation of two kinetic processes: i) reduction of riddelliine N-oxide to riddelliine, resulting in a less than linear increase in the $AUC_{0-24h, RID}$ with increasing dose of the N-oxide, and ii) clearance of riddelliine, resulting in more than linear increase in the $AUC_{0-24h, RID}$ upon dosing the PA itself. Both effects result in an increase in the $REP_{RIDO \text{ to } RID}$, calculated as the $AUC_{0-24h, RID}$ upon dosing the N-oxide (decreasing with the dose) divided by the $AUC_{0-24h, RID}$ upon dosing the PA (increasing with dose) [7]. These data clearly show that REP varies with dose when kinetics saturate, and they might saturate at different dose for different congeners [9].

Effect of species differences

Building similar PBK models for senecionine and its N-oxide, for not only rats but also humans, allowed

Figure 1



a) Riddelliine blood concentration-time curves as simulated by PBK modeling following an oral dosage of riddelliine (dashed line) or riddelliine N-oxide (solid line) in rat, and b) $REP_{PANO \text{ to } PA}$ value of riddelliine N-oxide compared to riddelliine ($REP_{RIDO \text{ to } RID}$) as derived using PBK modeling [7] or calculated from existing animal data by Xia et al. [8]. Graphs are extracted from Widjaja et al., 2022 [7]. PBK, physiologically based kinetic; REP, relative potency.

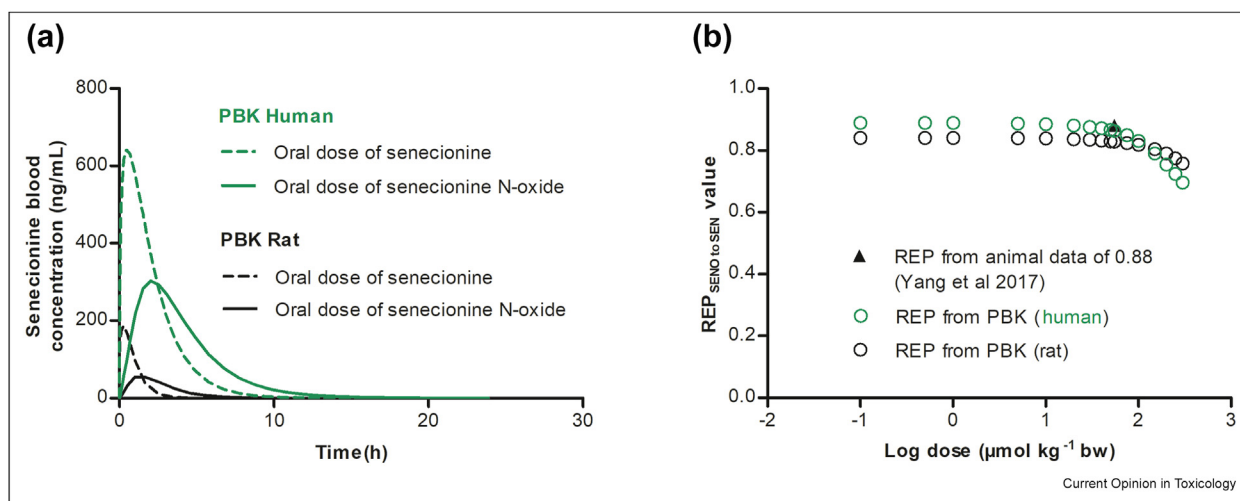
evaluating species differences and also the NAMs approach, since also for this PA and its N-oxide in vivo data to define a $REP_{\text{PANO to PA}}$ in rats is available [10]. Figure 2a presents the concentration-time curves for rat and human for senecionine N-oxide and its parent PA, and Figure 2b shows the $REP_{\text{SENO to SEN}}$ derived from the corresponding $AUC_{0-24h, \text{ SEN}}$ values at different dose levels. The results obtained reveal that i) the predicted $REP_{\text{SENO to SEN}}$ of 0.88 at the dose of the in vivo study [11] is in line with the predicted value of 0.84 [10] calculated by the NAMs approach, ii) also for this PA, $REP_{\text{PANO to PA}}$ decreases with increasing dose and is higher at low level exposure than the value obtained at the experimental dose applied in the rat study, and iii) species differences between rats and human are predicted to be limited, with $REP_{\text{PANO to PA}}$ at realistic dose for human risk assessment, amounting to 0.84 and 0.89 for rats and humans, respectively [10].

Effect of endpoint used

In the NAMs applied, $REP_{\text{PANO to PA}}$ was calculated using the $AUC_{0-24h, \text{ PA}}$ for the parent PA as the endpoint. The data for riddelliine N-oxide and senecionine N-oxide discussed above revealed that the predicted $REP_{\text{PANO to PA}}$ was in line with the REP derived from in vivo experimental data. For senecionine N-oxide, the experimental data also allowed calculating $REP_{\text{SENO to SEN}}$ based on the amount of pyrrole-protein adducts formed [11], resulting in 0.61. This was lower than the 0.88 obtained based on the $AUC_{0-24h, \text{ PA}}$ [11], and thus $REP_{\text{PANO to PA}}$ varied with the endpoint used.

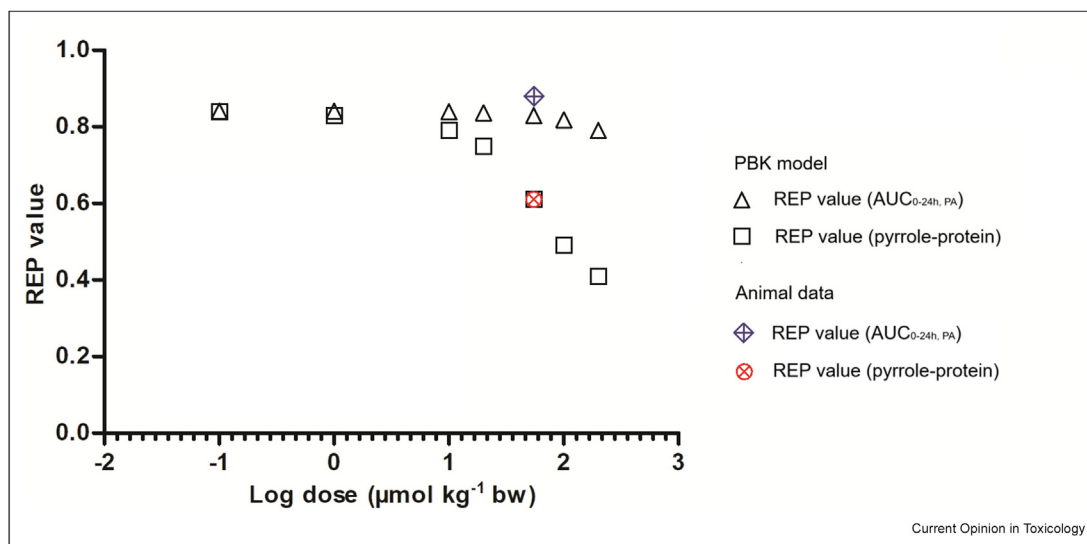
Extending the PBK model to predict the amount of pyrrole-protein adducts formed and including the scavenging of reactive pyrrole intermediate by reduced glutathione (GSH), revealed that this did not influence the $REP_{\text{PANO to PA}}$ derived from the $AUC_{0-24h, \text{ PA}}$, but could explain the lower $REP_{\text{PANO to PA}}$ at high dose levels. At higher doses, especially upon dosing the PA and not when dosing the PA-N-oxide, GSH depletion resulted in relatively higher level of pyrrole-protein adducts formed since scavenging of the reactive pyrrole intermediates by GSH was reduced [12]. At low dose, GSH depletion does not occur, and $REP_{\text{PANO to PA}}$ calculated based on the $AUC_{0-24h, \text{ PA}}$ becomes similar to the one based on the amount of pyrrole-protein adducts (Figure 3). Only at high dose of the PA where GSH levels are depleted [13–15], is the $REP_{\text{PANO to PA}}$ calculated based on the pyrrole-protein adduct levels lower than the one based on the $AUC_{0-24h, \text{ PA}}$. GSH depletion is more readily observed upon dosing the PA than upon dosing the N-oxide because dosing the N-oxide results in lower concentrations of the PA (Figures 1a and 2a) and thus lower chances on GSH depletion are observed. More GSH depletion upon dosing the PA results in higher pyrrole-protein adduct formation when dosing the PA than when dosing an equimolar dose of the N-oxide, resulting in a lower $REP_{\text{PANO to PA}}$ when calculated based on pyrrole-protein adducts formed. The results obtained also reveal that at low doses relevant for human dietary intake, $REP_{\text{PANO to PA}}$ obtained based on the two endpoints are similar, and the $AUC_{0-24h, \text{ PA}}$ is an adequate endpoint to define $REP_{\text{PANO to PA}}$.

Figure 2



a) Senecionine blood concentration–time curves as simulated by PBK modeling following an oral dosage of senecionine (dashed line) or senecionine N-oxide (solid line) in human (green) and rat (black), b) REP value for senecionine N-oxide relative to senecionine ($REP_{\text{SENO to SEN}}$) with increasing dose level as simulated by PBK modeling for human and rat, also presenting the REP value derived from animal data taken from Yang et al. [11]. Graphs were extracted from a previous publication by Widjaja-van den Ende et al. [10]. PBK, physiologically based kinetic; REP, relative potency; SEN; senecionine N-oxide; SEN, senecionine N-oxide.

Figure 3



REP_{SENO to SEN} when simulated with the PBK model based on either the AUC_{0-24h, PA} or the pyrrole-protein adducts compared to values obtained from animal data reported by Yang et al. [11]. This graph was extracted from Widjaja-van den Ende et al. [12]. AUC, area under the concentration–time curve; PBK, physiologically based kinetic; REP, relative potency; SENO, senecionine N-oxide; PA, pyrrolizidine alkaloid.

Effect of interindividual variability

REPs defined based on *in vitro* assays [16,17] generally do not consider differences in *in vivo* kinetics such as interindividual differences in the actual human population. PBK modeling coupled to Monte Carlo simulation allows measuring the consequences of interindividual variability in kinetics on REP_{PANO to PA}. To this end, the characteristics of the distributions from which the Monte Carlo simulation samples the kinetic constant to describe different individuals were defined based on both literature and experimental data. Experimental data on interindividual variability were defined for the metabolic kinetic parameters for PA-N-oxide reduction by fecal microbiota or liver enzymes and PA clearance by liver enzymes, using samples from 25 or 30 individuals and Bayesian statistics to interpret the data and define the distributions. Figure 4 shows the results obtained and reveals that REP_{PANO to PA} for riddelliine N-oxide relative to riddelliine at low dose may vary from 0.71 to 0.97, with a mean value of 0.87, due to interindividual differences in kinetics [18]. Using the 95th percentile of the distribution for a worst-case estimate in risk assessment yields 0.97.

Effect of chemical structure

Table 1 presents REP_{PANO to PA} obtained by the same NAM approach for other PA-N-oxides (Figure 5) at low dose [9,19]. This reveals that, in line with the assumption underlying the toxic equivalency concept, differences in chemical structure result in different REP_{PANO to PA}. At low doses, where the influences of

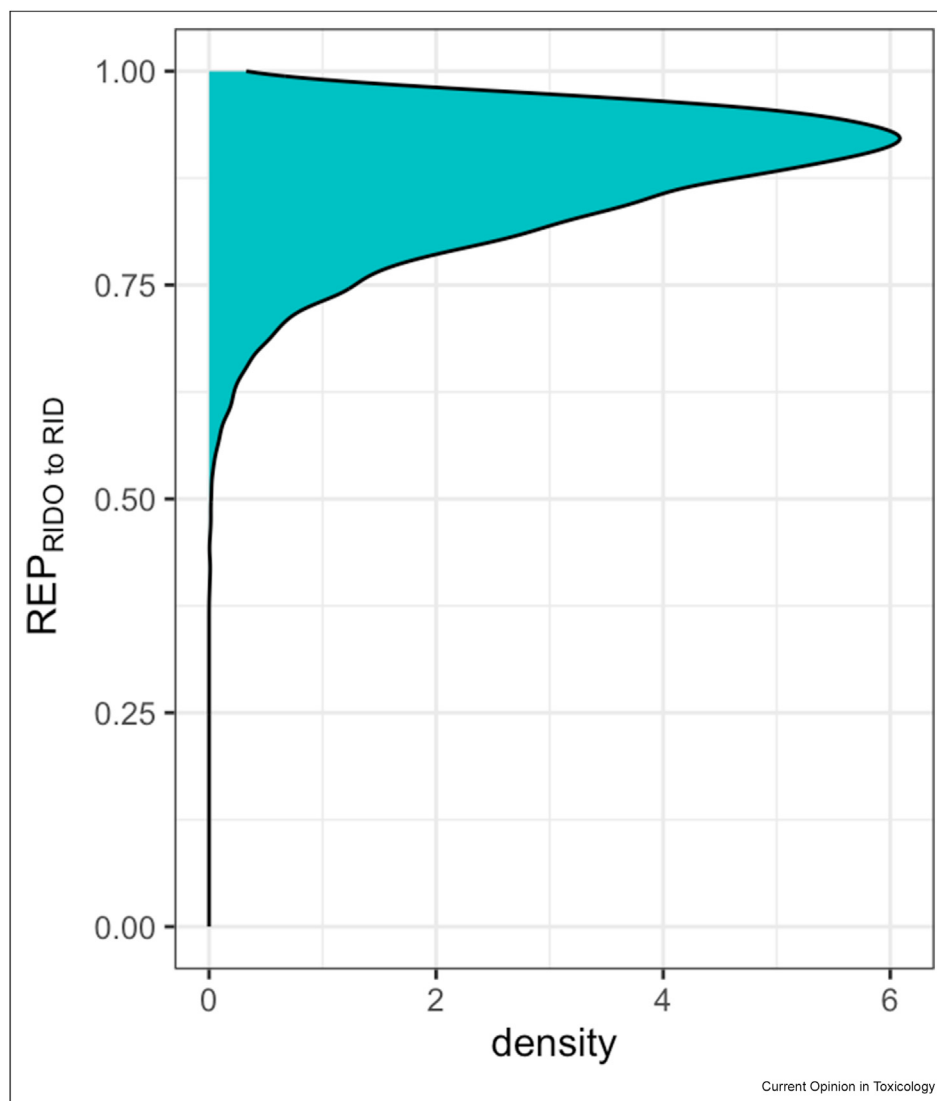
dose and species differences were limited, influences of chemical structure are substantial, as are influences of interindividual differences. To be used in combined risk assessment, REP_{PANO to PA} is multiplied by the REP_{PA to RID} to obtain REP_{PANO to RID}, which allows calculation of PA-N-oxide dose levels in riddelliine equivalents. Table 1 presents the REP_{PANO to RID} thus obtained and reveals these values to be 1.09- to 2.33-fold lower than the corresponding interim REP_{PANO to RID} proposed for these PA-N-oxides, assuming PA-N-oxides to be equally toxic as the corresponding PAs [20].

Implications for other groups of compounds

It is of interest to consider the implications of the results obtained when using PBK modeling to define REP values for the PA-N-oxides, for the REP values currently in use for dioxins [21–23], and proposed for PFAS [4,24,25].

A first lesson learned is that when REP values are quantified based on *in vitro* bioassays, such as micronucleus assay [17] or γ H2AX assay [16] for PA-N-oxides, or in some cases, the DR-CALUX assay for activation of the Ah receptor for dioxins, the resulting REP values reflect toxicodynamics differences only. These values do not account for toxicokinetic differences. This is especially true for dioxins, although most REP values for dioxins are still based on *in vivo* data rather than *in vitro* assays like CALUX. This shortcoming could be solved by using PBK models to translate the concentration–response curves obtained in the

Figure 4



Distribution of $REP_{RIDO \text{ to } RID}$, calculated based on $AUC_{0-24h, PA}$ when simulated with the PBK model for the human population at $1 \mu\text{mol/kg bw}$ riddelliine N-oxide or an equimolar dose of riddelliine. This graph was extracted from Widjaja-van den Ende et al. [18]. AUC, area under the concentration–time curve; PBK, physiologically based kinetic; REP, relative potency; RIDO, riddelliine N-oxide; RID, riddelliine.

in vitro bioassay to in vivo dose–response curves by PBK modeling-facilitated reverse dosimetry [26]. REPs could subsequently be defined based on the predicted in vivo dose that produces a specific response in 50% of the population (ED50 values), instead of based on the in vitro concentration where 50% of the maximal response is observed (EC50 values). Differences between in vitro effective concentrations and in vivo effective doses for related compounds may be substantial. This is for example illustrated by data reported for the in vitro and in vivo developmental toxicity of a series of phenol derivatives [27] (Figure 6), where especially the different in vivo kinetics for the p-

heptyloxyphenol compared to the other congeners results in a substantial difference between the in vitro embryonic stem cell test (EST)-based REPs and the in vivo observed and predicted REPs.

When it can be argued that differences in kinetics between congeners within a group are small, as may be the case for a series of closely related dioxins with comparable physicochemical and kinetic characteristics, the influence of kinetics may be limited. However, for compounds with different physicochemical and kinetic characteristics, these differences can substantially influence REP.

Table 1 REP_{PANO to PA} taken from Widjaja-van den Ende et al. [7,9,10] and from Alhejji et al. (submitted) [19], interim REP_{PA to RID} defined by Merz and Schrenk [20], and REP_{PANO to RID} to be used in combined risk assessment at low dose levels, obtained by multiplying the REP_{PANO to PA} with the corresponding REP_{PA to RID}.

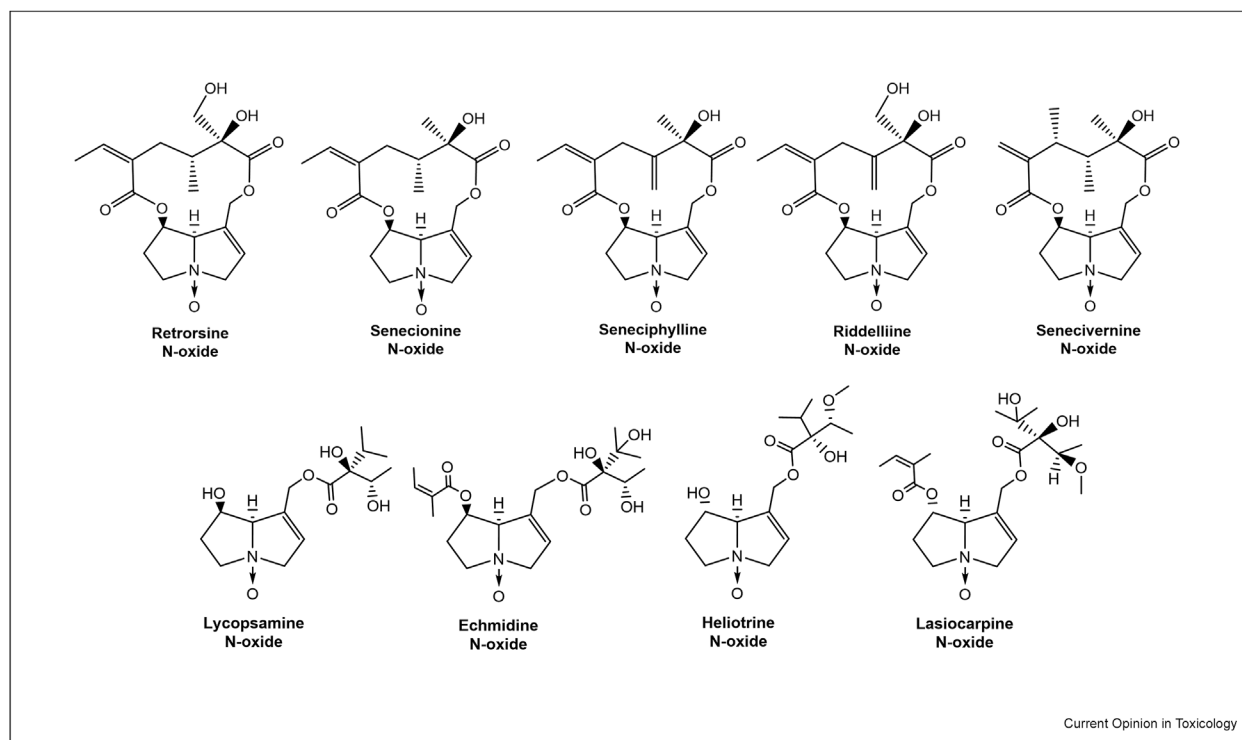
Compound	Group	REP _{PANO to PA} (Widjaja-van den Ende et al. [7,10,12,18]; Alhejji et al. [9,19])	REP _{PA to RID} ^a (Merz and Schrenk [20])	REP _{PANO to RID} (=REP _{PANO to PA} × REP _{PA to RID})	Fold difference ^b
Retrorsine (N-oxide)	7R, cyclic, diester	0.92	1	0.92	1.09
Senecionine (N-oxide)	7R, cyclic, diester	0.84	1	0.84	1.19
Seneciophylline (N-oxide)	7R, cyclic, diester	0.81	1	0.81	1.23
Riddelliine (N-oxide)	7R, cyclic, diester	0.78	1	0.78	1.28
Senecivernine (N-oxide)	7R, cyclic, diester	0.68	1	0.68	1.47
Lasiocarpine (N-oxide)	7S, open, diester	0.43	1	0.43	2.33
Echimidine (N-oxide)	7R, open, diester	0.56	0.1	0.056	1.79
Heliotrine (N-oxide)	7S, monoester	0.43	0.3	0.129	2.33
Lycopsamine (N-oxide)	7R, monoester	0.63	0.01	0.0063	1.59

PA, pyrrolizidine alkaloid; REP, relative potency; RID, riddelliine.

^a The values of REP_{PA to RID} and REP_{PANO to RID} in this publication are assumed to be the same because PA-N-oxides are assumed to have the same potency as their parent PAs. But only the REP_{PA to RID} are taken in this calculation.

^b The fold difference is calculated based on this equation: REP_{PANO to RID} (from Merz and Schrenk, which is equal to REP_{PA to RID} due to worst case scenario assumption) divided by REP_{PANO to RID} (obtained in current approach).

Figure 5

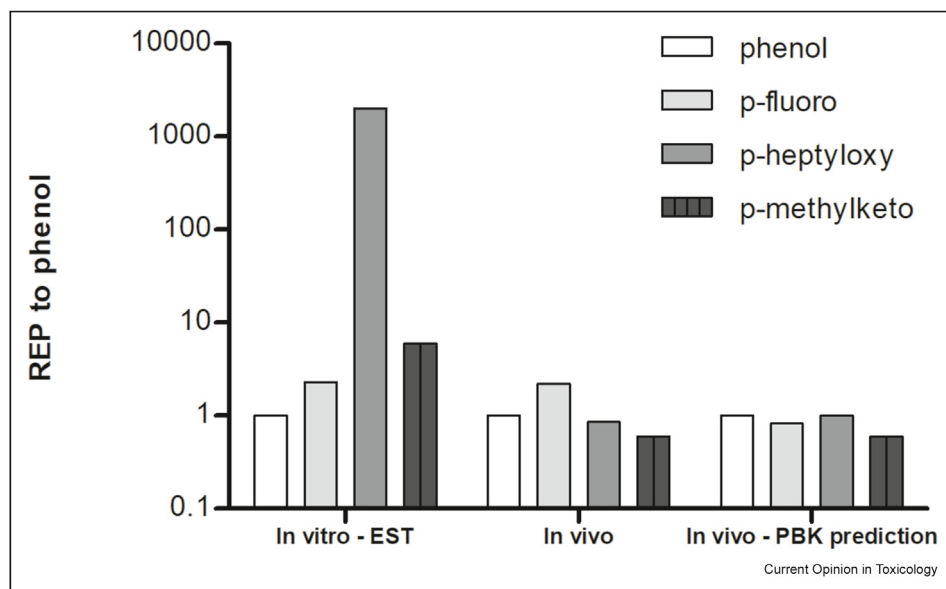


Chemical structures of various PA-N-oxides selected in Table 1. PA-N-oxides, pyrrolizidine alkaloid N-oxides.

Quantifying REP in in vivo studies may overcome the issue of not taking differences in in vivo kinetics into account. However, the second lesson learned is that this should be done at low dose where kinetics are not saturated. At high dose, differences in kinetics between

congeners may result in differences in the dose at which saturation of clearance or bioactivation occurs, which will affect differences in REP. This may imply that REP determined in animal studies at high dose are not adequate for low dose human risk assessment. It is

Figure 6



REP of p-substituted phenols compared to phenol as reference compound with REP of 1. REP values were extracted from Strikwold et al. [27] and were derived from the in vitro EST assay, in vivo data from Kavlock [28], and the in vivo prediction obtained based on PBK modeling-facilitated reverse dosimetry of the in vitro EST data [27]. PBK, physiologically based kinetic; REP, relative potency.

worth emphasizing that the term ‘dose’ here refers oral dose in a single administration, which may be different than the internal ‘dose’ or body burden for persistent, bioaccumulative, and toxic substances.

Finally, use of an endpoint irrelevant for human risk assessment, such as when defining REP values for PFAS based on liver toxicity while the adverse effects on which the TWI is based on is immunotoxicity [29] also raises questions on the validity of such values for human risk assessment. The REPs for PA-N-oxides are relevant because the toxic effects are initiated by the formation of PAs that are bioactivated into the same toxic pyrrole moieties, as well as for dioxins because the toxic effects are all initiated by activation of the Ah receptor. In contrast, PFAS activates multiple different receptors, and the results differ depending on the context of the study [30,31], where consequently, use of a ‘class’ approach might be more suitable than ‘REPs’ approach for risk assessment [32].

Discussion

From the overview presented, it becomes clear that when defining REP, it is important that the conditions and endpoint used match the human exposure. This implies the use of relevant dose and endpoint, and consideration of differences in kinetics, interspecies, and interindividual variability.

Additionally, performing studies on the influence of dose, species, endpoint used, and interindividual

differences based on in vivo animal experiments is unrealistic. This requires high number of animals, studies on humans will generally not be possible, detection limits for the relevant endpoints are often not sensitive enough at low dose, and animal models may be less relevant to evaluate effects in human. Using in vitro assays, on the other hand, ignores differences in in vivo kinetics amongst other limitations [33]. Using PBK modeling as NAM can help to overcome these limitations by either translating in vitro data to the human in vivo situation, or by defining relevant in vivo concentrations of parent compounds or intermediates relevant for the ultimate effect, based on which REP can be defined. It is clear that REP depends on differences in both toxicodynamics and toxicokinetics, and that NAMs can take such differences into account in the examples discussed in this review, but this requires evaluation on a case-by-case basis.

Declaration of Competing Interest

The authors declare that they have no known competing financial interests or personal relationships that could have appeared to influence the work reported in this paper.

Acknowledgements

I would like to express my deepest gratitude to Ivonne M. C. M. Rietjens, whose guidance, wisdom, and unwavering support have been invaluable throughout this work. Your patience, kindness, and unmatched work ethic continue to inspire me every day, and I am beyond grateful to have you as my mentor.

Data availability

No data was used for the research described in the article.

References

Papers of particular interest, published within the period of review, have been highlighted as:

- of special interest
- of outstanding interest

1. Ring C, Blanchette A, Klaren WD, Fitch S, Haws L, Wheeler MW, *et al.*: **A multi-tiered hierarchical Bayesian approach to derive toxic equivalency factors for dioxin-like compounds.** *Regul Toxicol Pharmacol* 2023, **143**, 105464.
2. Schmidt S: **Truth in the serum? Estimating PFAS relative potency for human risk assessment.** *Environ Health Perspect* 2022, **130**, 094001.
3. Scippo M-L, Eppe G, De Pauw E, Maghuin-Rogister G: **DR-CALUX® screening of food samples: evaluation of the quantitative approach to measure dioxin, furans and dioxin-like PCBs.** *Talanta* 2004, **63**:1193–1202.
4. Bil W, Ehrlich V, Chen G, Vandebriel R, Zeilmaker M, Luijten M, *et al.*: **Internal relative potency factors based on immunotoxicity for the risk assessment of mixtures of per-and polyfluoroalkyl substances (PFAS) in human biomonitoring.** *Environ Int* 2023, **171**, 107727.
5. Chain EPoCitF, Schrenk D, Bignami M, Bodin L, Chipman JK, del Mazo J, *et al.*: **Risk to human health related to the presence of perfluoroalkyl substances in food.** *EFSA J* 2020, **18**, e06223.
6. EFSA Knutsen HK, Alexander J, Barregård L, Bignami M, Bruschweiler B, *et al.*: **Risks for human health related to the presence of pyrrolizidine alkaloids in honey, tea, herbal infusions and food supplements.** *EFSA J* 2017, **15**, e04908.
7. Widjaja-van den Ende F, Wesseling S, Rietjens IMCM: **Physiologically based kinetic modelling predicts the in vivo relative potency of riddelliine N-oxide compared to riddelliine in rat to be dose dependent.** *Arch Toxicol* 2022, **96**:135–151.
Note: This study highlights the influence of dose to REP value.
8. Xia Q, Zhao Y, Von Tungeln LS, Doerge DR, Lin G, Cai L, *et al.*: **Pyrrolizidine alkaloid-derived DNA adducts as a common biological biomarker of pyrrolizidine alkaloid-induced tumorigenicity.** *Chem Res Toxicol* 2013, **26**:1384–1396.
9. Alhejji Y, Widjaja-van den Ende F, Tian S, Hoekstra T, Wesseling S, Rietjens IMCM: **In vitro-in silico study on the influence of dose, fraction bioactivated and endpoint used on the relative potency value of pyrrolizidine alkaloid N-oxides compared to parent pyrrolizidine alkaloids.** *Curr Res Toxicol* 2024, 100160.
Note: This study highlights the influence of chemical structures to REP value, within the macrocyclic diester group.
10. Widjaja-van den Ende F, Alhejji Y, Yangchen J, Wesseling S, Rietjens IMCM: **Physiologically-based kinetic modeling predicts similar in vivo relative potency of senecionine N-oxide for rat and human at realistic low exposure levels.** *Mol Nutr Food Res* 2023, **67**, 2200293.
Note: This study highlights the influence of species to REP value.
11. Yang M, Ruan J, Gao H, Li N, Ma J, Xue J, *et al.*: **First evidence of pyrrolizidine alkaloid N-oxide-induced hepatic sinusoidal obstruction syndrome in humans.** *Arch Toxicol* 2017, **91**:3913–3925.
12. Widjaja-van den Ende F, Zheng L, Wesseling S, Rietjens IMCM: **Physiologically based kinetic modeling of senecionine N-oxide in rats as a new approach methodology to define the effects of dose and endpoint used on relative potency values of pyrrolizidine alkaloid N-oxides.** *Front Pharmacol* 2023, **14**.
Note: This study highlights the influence of endpoint to REP value.
13. Chen Y, Ji L, Wang H, Wang Z: **Intracellular glutathione plays important roles in pyrrolizidine alkaloids-induced growth inhibition on hepatocytes.** *Environ Toxicol Pharmacol* 2009, **28**:357–362.
14. Neuman MG, Jia AY, Steenkamp V: **Senecio latifolius induces in vitro hepatocytotoxicity in a human cell line.** *Can J Physiol Pharmacol* 2007, **85**:1063–1075.
15. Griffin DS, Segall H: **Role of cellular calcium homeostasis in toxic liver injury induced by the pyrrolizidine alkaloid senecionine and the alkenal trans-4-OH-2-hexenal.** *J Biochem Toxicol* 1987, **2**:155–167.
16. Louise J, Rijkers D, Stoopen G, Holleboom WJ, Delagrangé M, Molthof E, *et al.*: **Determination of genotoxic potencies of pyrrolizidine alkaloids in HepaRG cells using the γ H2AX assay.** *Food Chem Toxicol* 2019, **131**, 110532.
17. Allemang A, Mahony C, Lester C, Pfuhrer S: **Relative potency of fifteen pyrrolizidine alkaloids to induce DNA damage as measured by micronucleus induction in HepaRG human liver cells.** *Food Chem Toxicol* 2018, **121**:72–81.
18. Widjaja-van den Ende F, van Boekel M, Davis C, Wesseling S, Rietjens IMCM: **Quantifying the effect of human interindividual kinetic differences on the relative potency value for riddelliine N-oxide at low dose levels by a new approach methodology.** *Regul Toxicol Pharmacol* 2025, **156**, 105767.
Note: This study highlights the influence of interindividual human variability to REP value.
19. Alhejji Y, Widjaja-van den Ende F, Wesseling S, Rietjens IMCM: **Predicting the in vivo relative potency values for open-chain diester and monoester pyrrolizidine alkaloids N-oxides by an in vitro-in silico new approach methodology.** [Submitted].
Note: This study highlights the influence of chemical structures to REP value, within the monoester and open chain diester group.
20. Merz K-H, Schrenk D: **Interim relative potency factors for the toxicological risk assessment of pyrrolizidine alkaloids in food and herbal medicines.** *Toxicol Lett* 2016, **263**:44–57.
21. Van den Berg M, Birnbaum LS, Denison M, De Vito M, Farland W, Feeley M, *et al.*: **The 2005 World Health Organization reevaluation of human and mammalian toxic equivalency factors for dioxins and dioxin-like compounds.** *Toxicol Sci* 2006, **93**:223–241.
22. van Ede KI, van Duursen MB, van den Berg M: **Evaluation of relative effect potencies (REPs) for dioxin-like compounds to derive systemic or human-specific TEFs to improve human risk assessment.** *Arch Toxicol* 2016, **90**:1293–1305.
23. Van den Berg M, Birnbaum L, Bosveld A, Brunström B, Cook P, Feeley M, *et al.*: **Toxic equivalency factors (TEFs) for PCBs, PCDDs, PCDFs for humans and wildlife.** *Environ Health Perspect* 1998, **106**:775–792.
24. Bil W, Zeilmaker M, Fragki S, Lijzen J, Verbruggen E, Bokkers B: **Risk assessment of per-and polyfluoroalkyl substance mixtures: a relative potency factor approach.** *Environ Toxicol Chem* 2021, **40**:859–870.
25. Bil W, Zeilmaker MJ, Bokkers BG: **Internal relative potency factors for the risk assessment of mixtures of per-and polyfluoroalkyl substances (PFAS) in human biomonitoring.** *Environ Health Perspect* 2022, **130**, 077005.
26. Louise J, Beekmann K, Rietjens IMCM: **Use of physiologically based kinetic modeling-based reverse dosimetry to predict in vivo toxicity from in vitro data.** *Chem Res Toxicol* 2017, **30**:114–125.
27. Strikwold M, Spenkelink B, de Haan LH, Woutersen RA, Punt A, Rietjens IMCM: **Integrating in vitro data and physiologically based kinetic (PBK) modelling to assess the in vivo potential developmental toxicity of a series of phenols.** *Arch Toxicol* 2017, **91**:2119–2133.
28. Kavlock RJ: **Structure-activity relationships in the developmental toxicity of substituted phenols: in vivo effects.** *Teratology* 1990, **41**:43–59.
29. Corsini E, Iulini M, Galbiati V, Maddalon A, Pappalardo F, Russo G, *et al.*: **EFSA Project on the use of NAMs to explore the immunotoxicity of PFAS.** *EFSA Support Pub* 2024, **21**(8):8926E.
30. Behr A-C, Plinsch C, Braeuning A, Buhke T: **Activation of human nuclear receptors by perfluoroalkylated substances (PFAS).** *Toxicol Vitro* 2020, **62**, 104700.

31. Houck KA, Patlewicz G, Richard AM, Williams AJ, Shobair MA, Smeltz M, *et al.*: **Bioactivity profiling of per-and polyfluoroalkyl substances (PFAS) identifies potential toxicity pathways related to molecular structure.** *Toxicology* 2021, **457**, 152789.
32. Kwiatkowski CF, Andrews DQ, Birnbaum LS, Bruton TA, DeWitt JC, Knappe DR, *et al.*: **Scientific basis for managing PFAS as a chemical class.** *Environ Sci Technol Lett* 2020, **7**: 532–543.
33. Blaauboer BJ: **The contribution of in vitro toxicity data in hazard and risk assessment: current limitations and future perspectives.** *Toxicol Lett* 2008, **180**:81–84.